J Mater Sci: Mater Med (2008) 19:3211–3220
DOI 10.1007/s10856-008-3451-0

Formation of hydroxyapatite coating using novel chemo-biomimetic method

Jianhui Xie · Ben Li Luan

Received: 5 December 2006 / Accepted: 8 April 2008 / Published online: 2 May 2008

Abstract A novel chemo-biomimetic method was developed to deposit hydroxyapatite (HA), simulating the porous nano-scale structure and chemical composition of natural bone. Electrochemical activation in NaOH solution, a prerequisite process to heterogeneously nucleate hydroxyapatite in this investigation, creates nano-scale porous structure on the surface of Ti6Al4V alloy. XPS analysis confirmed that the surface of activated Ti6Al4V substrate converted to TiO_2 during activation, existing in the form of hydrated TiO_2. Benefiting from the biocompatible top-layer of hydrated TiO_2 and the favorable alkaline surface chemistry created through the electrochemical activation, the HA coating nucleates heterogeneously and grows continuously on the activated substrate resembling the nano-scale porous bone-like structure. The coating was characterized using XRD, SEM/FESEM/EDX, TEM and FTIR, and was confirmed as pure hydroxyapatite. A coating thickness of 50 μm was achieved, which is preferable and acceptable for medical implant application to promote bone ingrowth, thus enhancing fixation and biocompatibility of implant surface.

1 Introduction

The prevalence of thigh pain (reported of up to 26% [1, 2]) after total hip replacement remains an unacceptable complaint by patients. The cause is probably due to a number of factors including unstable fibrous fixation, the mismatch between the moduli of elasticity for the prosthesis material and bone, fatigue fracture, relative motion across the interface between the implants and the surrounding tissues due to excessive stress at the implant/body tissue interfaces, and endosteal irritation [3–4]. Furthermore, materials implanted in vivo essentially have direct contact with human body through the interface between the implant surface and bones, tissues and extracellular body fluids. The surface of the implant therefore plays a very important role related to surface chemistry, topography and micro/nano structure, and tribological properties. This requires a surface modification to promote the ingrowth of human bone into the implanted biomaterials, more preferentially to form a natural and smooth connection between bone and implant.

Titanium and titanium alloys, bioinert materials due to a stable oxide layer at the surface [5–7], have been extensively investigated and applied as an implanting material due to their combined properties of corrosion resistance and biocompatibility with mechanical performance [8]. But these artificial materials implanted are generally encapsulated by a soft fibrous tissue, leading to isolation from the surrounding bone and a weak bonding between implant and bone [8, 9]. The calcium phosphate ceramics, bioactive materials, on the other hand can promote osteoconductivity and create a direct chemical bonding between implant and surrounding bone [8]. Much attention has therefore been focused on ceramics which resemble the mineral phase in bone tissues, i.e. hydroxyapatite, octacalcium phosphate and tricalcium phosphate [8, 10–12]. To take advantage of the excellent characteristics of Ti-alloys and to avoid the isolating layer of soft tissue around the Ti implants, the growth of apatite coating onto the Ti-alloy is currently being extensively investigated [9, 12–19].

J. Xie · B. L. Luan (✉)
Integrated Manufacturing Technologies Institute (IMTI),
National Research Council Canada, 800 Collip Circle,
London, ON, Canada N6G 4X8
e-mail: ben.luan@nrc-cnrc.gc.ca

However, most of the techniques for apatite coating are line-of-sight dependant and/or involves high temperature. It is a tremendous challenge for any process that is line-of-sight in nature to produce uniform coating, particularly on complex geometries; As for processes that rely on high temperature, they cause decomposition of HA which leads to the formation of impurities such as tetracalcium phosphate ($Ca_4P_2O_9$), amorphous calcium phosphate, α- and/or β-tricalcium phosphate ($Ca_3(PO_4)_2$). These impurities are relatively unstable in the body fluids as compared to HA and the uneven surface formed due to the selective dissolution of these impurities may result in an accelerated wear caused by the roughening of the surface, and the debris will, in turn, make the wear a more severe issue.

Biomimetic [14–16] and chemical processes [20, 21] are neither line-of-sight dependant nor involve high temperature operation. Biomimetic coating is an approach that consists of the immersion of metal implants in simulated body fluids (SBF) at a physiologic temperature and pH. HA coating, the major component of bone, grows in a way similar to the natural bone growth in human body. This process produces HA coating with desirable properties such as high purity and bioactivity. However, achieving a reasonable coating thickness by the biomimetic method for practical applications takes a long time. As a result of the low solubility product of HA and the limited concentration range for the metastable phase, this operation is extremely difficult and may lead to local precipitation or uneven coatings. Such an intricate and long process can hardly be tolerated in the prostheses coating industry. Chemical processes produce coatings at low temperature and is not line-of-sight dependent. It is a process to produce HA coating based simply on chemical reaction. Theoretically, this process can produce a uniform coating with unlimited thickness on complex shapes. The deposition rate of chemical HA coating is significantly higher than the biomimetic process due to significantly higher and controllable solution composition. Unfortunately, little is known about its chemical reaction kinetics and the process is used mainly for producing HA powders.

In order to combine the advantages of biomimetic and chemical processes, extensive research was conducted in our laboratory to develop a novel process for coating of hydroxyapatite on Ti6Al4V alloy for orthopaedic applications. The novel approach presented in this communication is termed "chemo-biomimetic HA coating process" for two reasons: (1) the deposition is based on the conventional biomimetic process simulating the natural bone growth, and (2) chemical modifications were conducted to the substrate surface chemistry prior to HA deposition as well as to the composition of deposition solutions, more specifically, increased calcium and phosphate concentrations. Both modifications are designed to accelerate the deposition process.

The novelty of this coating method relies on: (1) the novel surface modification with nano-scale surface microstructure and favourable surface chemistry for the heterogeneous growth of hydroxyapatite coating, and (2) the very fast growth of the coating with novel coating composition. In this investigation, the surface was electrochemically activated in 10 M NaOH solution at room temperature with an application of voltage of 10 V for only 30 min. This activation resulted in nanometer scale porous surface microstructure, a bone-like structure [22]. In addition, the activated surface was in alkaline pH, which is a prerequisite and favourable condition for the heterogeneous growth of hydroxyapatite coating. While other researchers activated the surface of the substrate using a chemical method, in which a concentrated NaOH solution (5–10 M) was heated to elevated temperature either in the open atmosphere or in autoclave [23–26]. Followed the chemical activation is a drying process and heat treatment. All of these processes usually took long time to complete. To grow pure hydroxyapatite coating on the surface, rather than the decomposition caused by the only commercially available plasma spraying method, this novel method was able to grow 50 μm thick of coating in only 15 h. While the most commonly used biomimetic method in order to grow pure hydroxyapatite coating usually takes weeks, or sometimes months to produce reasonable thickness, e.g. 50 μm [27–29]. The concentration of the coating solution in this investigation was modified with Ca^{2+} and PO_4^{3-} five times of these used in the traditional biomimetic method, and the supersaturation of Ca^{2+} and PO_4^{3-} was able to hold with proper pH of the solution. With all the favourable conditions and replenishing the coating solution every 30 min, the coating thickness was linearly increased with the coating duration due to the almost constant growth rate in the almost constant concentration of the solution.

2 Experimental details

2.1 Materials and preparation of samples

A Ti6Al4V-ELI alloy (RMI Titanium Company, Mississauga, Canada) with a chemical composition (wt.%) of 0.12 O, 0.02 C, 0.08 N, 0.213 Fe, 6.16 Al, 3.92 V and balance Ti was chosen as the testing material. The specimens (10×10 mm^2) were cut from a rolled plate (1.7 mm thick), mechanically polished using SiC paper #400 and #600, and 9 μm Al_2O_3 paper.

A Ti wire was spot-welded to the polished sample for handling, and the polished samples were ultrasonically cleaned in acetone, ethanol and deionized water for 10 min each, separately. The clean specimens were then etched in a 0.2 vol.% HF + 0.4 vol.% HNO_3 acid solution for 10 min, rinsed thoroughly with deionized water, subjected

to ultrasonic cleaning for 10 min in deionized water and dried at room temperature. The specimens were ready for the further electrochemical activation treatment.

2.2 Electrochemical activation treatment of Ti6Al4V substrates

The electrochemical activation treatment of Ti6Al4V alloy prior to HA deposition was carried out at room temperature in a 10 M NaOH solution for 30 min. A constant voltage of 10 V was applied using HP E3610A DC power supply on the cleaned and etched samples (as working electrode). Two identical Ti6Al4V alloy plates (30×30 mm^2), equally distanced from the working electrode, were used as counter electrodes. After the electrochemical activation, the specimen was thoroughly rinsed using deionized water for subsequent apatite deposition.

2.3 The chemo-biomimetic method for coating hydroxyapatite

The apatite coating was formed in a solution with enhanced Ca^{2+} and HPO_4^{2-}concentrations by a factor of five, 5(Ca & P), shown in Table 1, as compared with the conventionally used simulated body fluid (SBF) and blood plasma. All the chemicals used for the solution are reagent grade, including NaCl (Fluka, ≥99.5%), $NaHCO_3$ (Sigma–Aldrich, ≥99.7%), KCl (Fisher, ≥99.6%), Na_2HPO_4 (Sigma–Aldrich, >99.0%), $MgCl_2 \cdot 6H_2O$ (Sigma–Aldrich, >99.0%), $CaCl_2 \cdot 6H_2O$ (Fisher, ≥99.5%), Na_2SO_4 (Anachemia, >99.0%). The solution pH was adjusted to 6.50 using HCl and TRIS (tris-hydroxymethyl aminomethan).

The coating process was conducted in 250 ml beakers with 175 ml solution, and the beakers were kept in a water bath at 37°C. The coating process was allowed to proceed for 30 min before new solution was replenished and this replenishing was conducted at 30 min intervals thereafter until completion of deposition. A separate coating process was allowed to proceed continuously for 5 h, without replenishment, to identify the effects of replenishment.

Table 1 Chemical composition (mM) of SBF, blood plasma and 5(Ca & P) solution

	Na^+	K^+	Mg^{2+}	Ca^{2+}	Cl^-	HCO_3^-	HPO_4^{2-}	SO_4^{2-}
5(Ca & P)	142.0	5.0	1.5	12.5	159.0	4.2	5.0	0.5
SBF	142.0	5.0	1.5	2.5	148.8	4.2	1.0	0.5
Blood plasma	142.0	5.0	1.5	2.5	103.0	27.0	1.0	0.5

2.4 Characterization of formed coating

The surface morphologies of hydroxyapatite coating on Ti6Al4V alloy were observed using Hitachi S-3500 SEM/EDX and Hitachi S-4500 field emission SEM (FESEM) equipped with an EDAXTM EDX system.

The nano grain size of formed hydroxyapatite coating was characterized using Philips CM20 Transmission Electron Microscope (TEM). The coating was scratched off the Ti6Al4V alloy substrate, dispensed in Ethanol, attached on a copper screen mesh for TEM analysis.

The coating was also scratched off the coated substrates and enough amount of powder was collected for XRD analysis. XRD analysis was carried out using a Bruker D8 diffractometer with Cu Kα radiation. The scan was conducted from 10° to 70° at a step of 0.02°.

The coatings were also analyzed using Perkin Elmer FTIR (Fourier Transform Infrared Spectroscopy) Instrument (Spectrum BX), with the scanning range set between 4,000 and 400 cm^{-1} for 216 scans for each sample.

X-ray photoelectron spectroscopy (XPS) was carried out on the activated Ti6Al4V alloy substrate with a Kratos AXIS Ultra spectrometer. XPS is a very surface sensitive analytical technique and, as such, provides elemental and chemical state data from the outer 5–10 nm of a surface. For this work, one set of analyses was carried out on each sample using a monochromatized Al Kα X-ray source. The analysis area was $\sim 700 \times 300$ μm in size. Survey (pass energy 160 eV) and high-resolution spectra (pass energy 20 eV) for Ti 2p, C 1s, and O 1s peaks were obtained for each sample.

3 Results and discussion

3.1 Activated Ti6Al4V alloy substrate

The XPS analysis shows that the surface of the activated Ti6Al4V substrate was completely converted to TiO_2 during activation (Fig. 1). The Ar^+ sputtering cleaned Ti6Al4V specimen (Fig. 1a) showed two peaks at the binding energies of 460.0 and 453.9 eV, attributable to Ti 2p1/2 and Ti 2p3/2 peaks, respectively. High resolution XPS spectrum of Ti 2p peaks (Fig. 1b) obtained for the electrochemically activated specimen showed no Ti 2p metal components, suggesting the formation of a thicker oxide layer on the surface (>5–10 nm). Both Ti 2p peaks corresponded to Ti^{4+} valence state, indicating that suboxides such as TiO, Ti_2O_3 or Ti_3O_5 were not present on the oxide surface. The O 1s peak (Fig. 1c) was fitted with three different components, lattice oxide (O^{2-}), hydroxide (physisorbed –OH), and water (chemisorbed H_2O). The specimen showed a major peak at 530.5 ± 0.3 eV, which

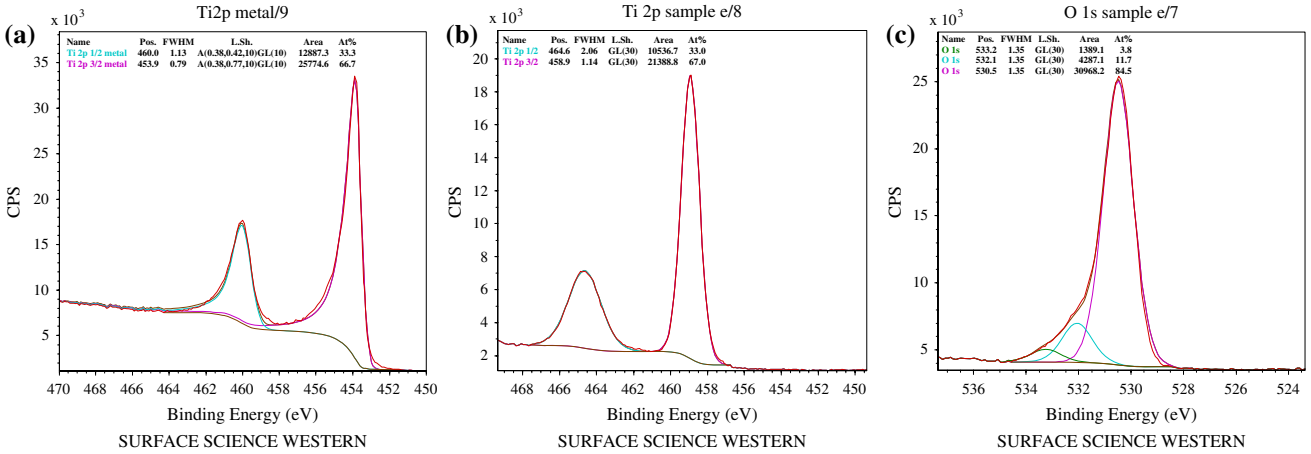

Fig. 1 High resolution XPS spectrum of Ti 2p for (**a**) Ar^+ sputtered and (**b**) electrochemically activated Ti6Al4V alloys, and of O 1s for (**c**) electrochemically activated Ti6Al4V alloy

is attributed to lattice oxide. Minor O 1s peaks at higher binding energies are attributable to hydroxides (532.0 eV) and chemisorbed H_2O (533.2 eV).

The electrochemically activated surface was verified as alkaline chemistry by surface pH measurement using pH indicators, shown in Table 2. These measurements revealed that the surface pH for etched Ti6Al4V alloy was in the range of 5.2–7.4; and that for the electrochemically activated Ti6Al4V alloy was equal or greater than 8.2, which is favorable for the formation of hydroxyapaptite.

3.2 Deposition of hydroxyapatite coating

3.2.1 Continuous coating process

In this chemo-biomimetic method, hydroxyapatite coating heterogeneously deposits on the Ti6Al4V alloy substrate due to both the nano-scale porous bone-like structure (With pore diameter of about 100 nm) (Fig. 2a) with top-layer of TiO_2 and favorable surface alkaline chemistry created through electrochemical activation in the NaOH solution. The formed coating, especially the initial layer of the

Table 2 Surface pH range of etched and electrochemically activated Ti6Al4V alloy

Indicators		Methyl orange	Bromocresol purple	m-Cresol purple	Phenolphthalein
Properties of indicators	pH range	3.2–4.4	5.2–6.8	1.2–2.8; 7.4–9.0	8.2–10.0
	Color change	Red to yellow	Yellow to purple	Red to yellow; yellow to purple	Color to pink
Reactions of samples to indicators	Etched	To yellow	To purple	To yellow	No change
	Activated			To purple	To pink

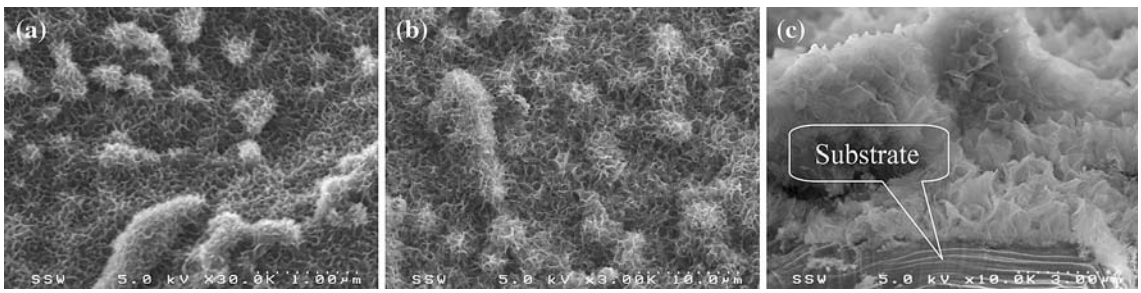

Fig. 2 FESEM presentations of (**a**) the surface of an activated Ti6Al4V alloy substrate, (**b**) surface morphology and (**c**) cross-section of the initial HA coating at 0.5 h of immersion in the solution

coating (Fig. 2b) has similar surface structure as the NaOH-activated substrate but with a larger pore diameter (about 1.0 μm) indicating a good potential for retaining proteins and antibiotics that are conducive to post-surgical healing. Cross-section of the initial coating (Fig. 2c) shows that the initial deposition forms a fine layer of coating with porous morphology, tightly attached to the substrate without coating loss along the edge of Ti6Al4V alloy substrate during the mechanical breakage of the sample.

The coating process on the activated Ti6Al4V alloy proceeds in the sequence of nucleation stage and growth stage. In the nucleation stage (Fig. 3a) apatite coating initially deposits on the activated surface through heterogeneous nucleation with spherical extrusions. The coating resembles porous bone-like structure and covers the whole surface of the substrate, even though only a short period of deposition is applied. At the growth stage, coating starts to grow in the valleys around the spherical features to create a leveled surface (Fig. 3b), which eventually demonstrates crystal-like morphologies at the fifth hour of deposition (Fig. 3c). It is shown from cross-section of the coating (Fig. 3d) that the continuous growth still creates fine porous structure throughout the coating. The cross-section of the coated Ti6Al4V was prepared by mechanically breaking the samples using a vise. It can be clearly seen from the fractured surface that even though a breakage is observable inside the coating, the initial layer of deposit still adheres well to the substrate, indicating a good interface bonding.

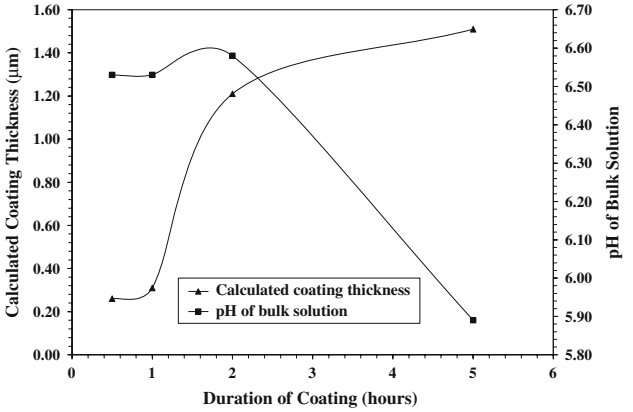

Fig. 4 Plot of calculated coating thickness as function of corresponding pH of bulk solution

Figure 4 shows calculated coating thickness and corresponding pH variation of bulk solution. The coating thickness was calculated from the weight gain of deposit on the substrate based on the full density of hydroxyapatite (3.16 g/cm^3). During the initial heterogeneous nucleation, the pH of the bulk solution is measured to be relatively unchanged. Accordingly, a relatively stable coating growth is maintained. At the growth stage, slightly increased pH at the second hour corresponds to a significant increase of coating thickness on the substrate. With the relatively high deposition rate of HA, chemicals in the solution are quickly depleted, leading to a significant reduction of pH in the

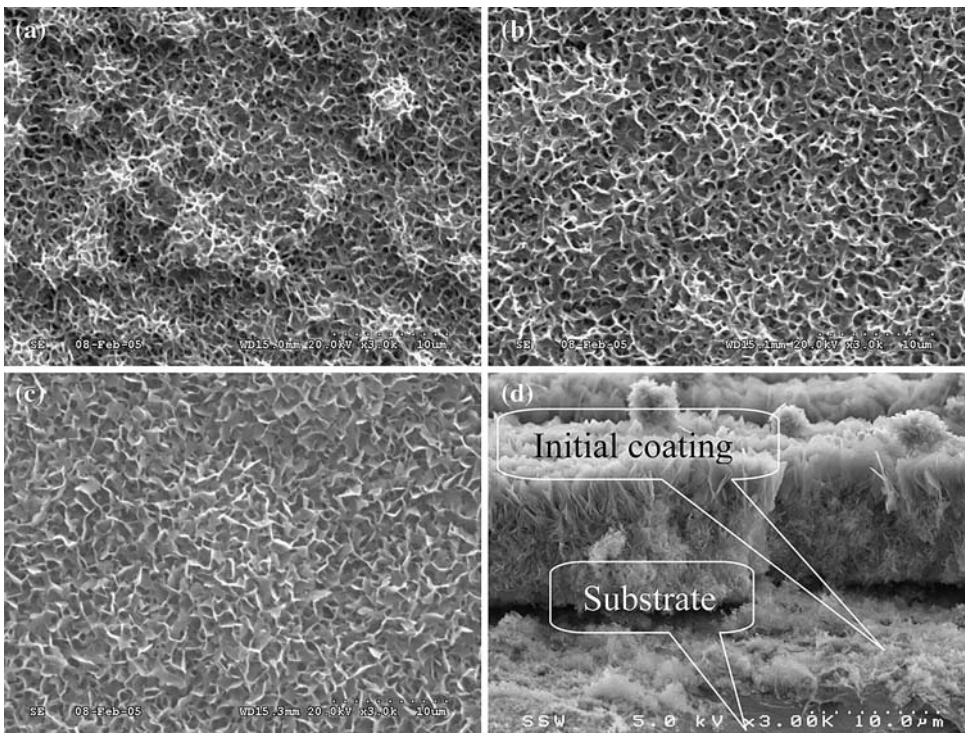

Fig. 3 Surface morphologies of apatite coating formed on activated Ti6Al4V alloy in the initial stage of (**a**) 0.5 h and the growth stage of (**b**) 2 h and (**c**) 5 h; (**d**) cross-section of coating at 5 h

solution and a reduced deposition rate. This indicates the need to replenish the solution at certain intervals.

3.2.2 *Replenishing solutions during coating processes*

The purpose of replenishing the solution is to investigate the deposition and growth of coating under "constant" concentration and pH of the solution, and maintain the deposition rate. The process was carried out by replenishing solution every half an hour with fresh solution, and necessary analysis was conducted on the coated samples retrieved at 0.5, 1, 2, 3, 4 and 5 h. The morphologies of coated Ti6Al4V substrates at different durations show that all coatings are bone-like structure and cover the whole surface of the Ti6Al4V alloy substrate. Coating morphology at one-half an hour (Fig. 5a) demonstrates that HA coating grows in a spherical shape across the surface, resulting in an uneven coating surface. Gradually the valleys around the spherical features are filled (Fig. 5b), resulting in a ball-like and relatively even coating surface with continued deposition. From the fourth hour (Fig. 5c), the coating grows to a certain thickness and starts to crack due to the accumulation of internal stress. Compared with the continuous coating process, the coatings in both processes are of similar bone-like morphology for the first 2 h, while the replenishing process maintains the dense and bone-like structure for the whole duration of coating with smaller pore size. The cross-section observation confirms that the coating is uniform on the edge, corner and the surface (Fig. 5d), attributable to the non line-of-sight nature of this method.

A linear relationship is observed (Fig. 6a) between the calculated coating thickness (from weight gain based on

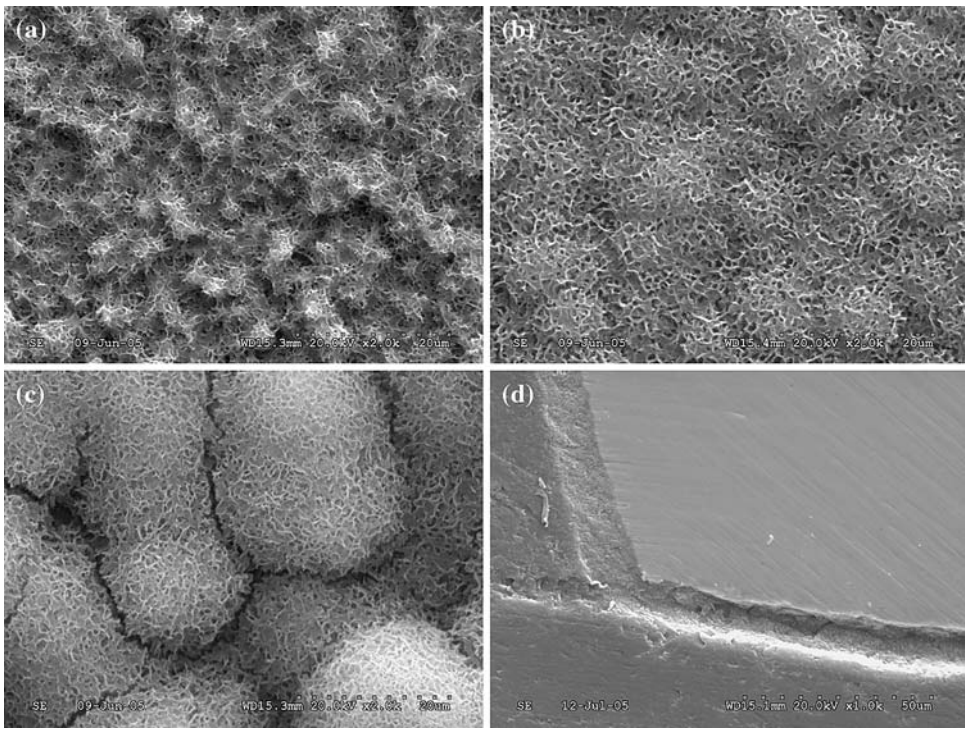

Fig. 5 Surface morphologies of HA coating at (**a**) 0.5, (**b**) 2 and (**c**) 4 h and (**d**) cross-section of 4 h of coating duration with replenishing solution every half an hour

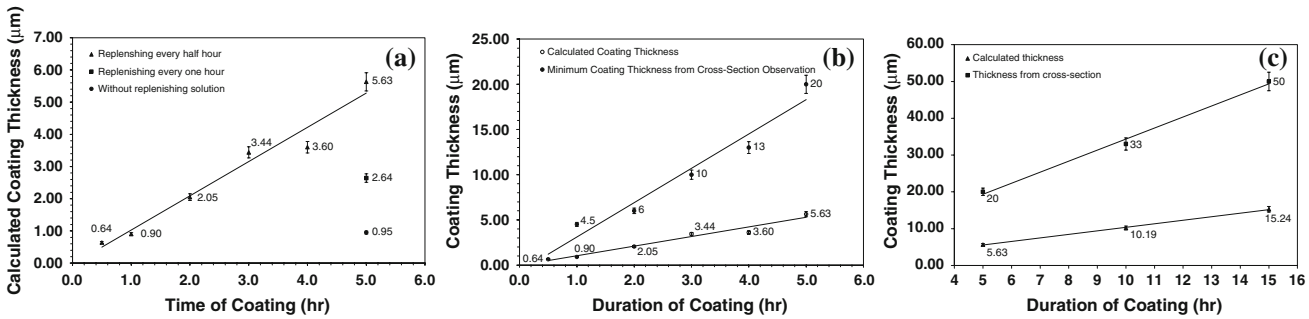

Fig. 6 (**a**) Effect of replenishing solution on the calculated coating thickness, comparison between the calculated and actual coating thickness for (**b**) short-term (5 h) and (**c**) long-term (15 h) coating processes

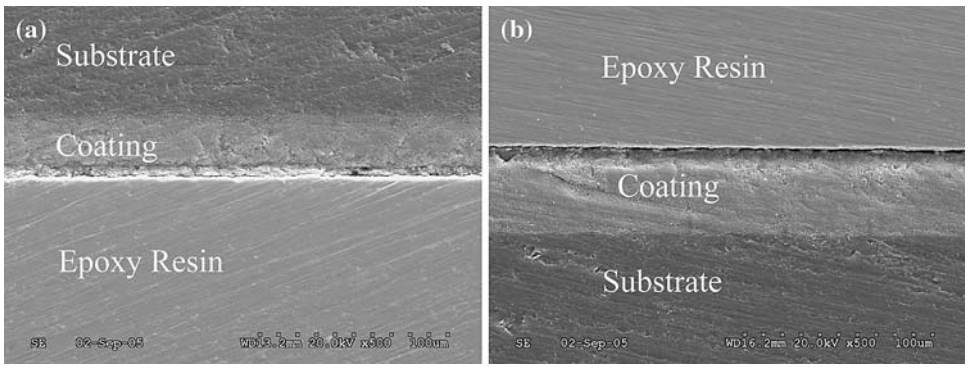

Fig. 7 Cross-section of coated Ti6Al4V alloy at (**b**) 10 and (**c**) 15 h of coating process

full density of hydroxyapatite) and the duration of coating. Comparing the coating thickness for a 1 h interval of replenishing and without replenishing for the 5-h coating process, replenishing solutions significantly increases the coating growth on the substrate. In other words, replenishing enables a steady growth of HA. It ought to be mentioned that the calculated coating thickness does not represent the actual coating thickness due to the large amount of porosities in the coating. The actual coating thickness was measured from the cross-section of the coated samples using SEM (Fig. 6b). Compared with the calculated coating thickness, the actual coating thickness is much greater and also linearly related to the duration of deposition.

To further confirm the linear growth of coating and the reliability of this coating process, long term deposition was carried out. The results confirm that a linear relationship between the coating thickness (actual) and the duration of coating process still exists (Fig. 6c). Coating thickness reaches 50 μm within 15 h, which is an acceptable thickness of hydroxyapatite coating for medical application. EDX analysis was conducted to define boundaries of the coating, and confirms that the thickness is around about 33 μm for the initial 10 h (Fig. 7a) and 50 μm for the 15 h (Fig. 7b) of deposition.

3.3 Characterization of formed coating

3.3.1 EDX analysis of coating

EDX line analysis conducted from the coating to the substrate (Fig. 8a) confirms that there is an initial layer with diffusion of Ti and Ca (about 2–3 μm), indicated by an arrow at the interface of substrate and the HA coating. This is possibly the result of the preferential reaction between TiO_2 and Ca^{2+} at the initial stage. The reaction possibly proceeds inside the pores (created by electrochemical activation) through the diffusion of Ca^{2+} into the pores, rather than the diffusion of Ti out of substrate.

During the electrochemical activation process in the alkaline solution, the naturally formed thin titanium oxide is easily dissolvable due to its reaction with OH^- to form $HTiO_3^-$. The subsequently exposed Ti is electrochemically oxidized in the alkaline solution possibly according to the following reaction (1):

$$\mathrm{Ti} + 3\mathrm{OH}^- - 3\mathrm{e} \rightarrow \mathrm{TiO_2} \cdot \mathrm{H_2O} + \frac{1}{2}\mathrm{H_2} \uparrow \quad (1)$$

Gas evolution was observed on the Ti6Al4V substrate, possibly the result of hydrogen formation. The XPS analysis (Fig. 1) shows that the O is mainly in the form

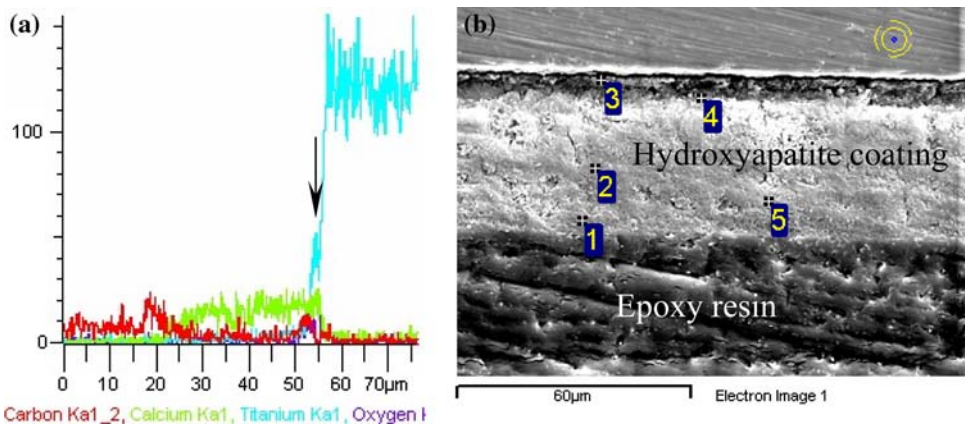

Fig. 8 (**a**) EDX line analysis to confirm the initial diffusion layer and (**b**) EDX point analysis of the coating

of lattice oxide (O^{2-}) with small amount of hydroxide (physisorbed OH^-) and water (chemisorbed H_2O), thus the surface of activated substrate is dominated by hydrated TiO_2 and possibly Ti-OH^- hydrogel layer. The nano-scale pores formed during activation process may also demonstrate a capillary effect, which absorbs and retains the NaOH solution in the pores, resulting in a higher local pH on the surface. In addition to the biocompatible TiO_2, the alkaline environment on the surface from both the capillary effect and Ti-OH^- layer is beneficial for the heterogeneous nucleation of hydroxyapatite on the surface, according to the following reaction (2):

$$10Ca^{2+} + 6PO_4^{3-} + 2OH^- \leftrightarrow Ca_{10}(PO_4)_6(OH)_2 \quad (2)$$

One of the main characteristics of metal oxides in aqueous solution is their point of zero charge (PZC), which represents the pH value of aqueous solution at which an immersed oxide surface has zero net charge. If the solution pH is greater than the pH at PZC of the metal oxide, the metal oxide is negatively charged; on the contrary, if the solution pH is lower than the pH at PZC of metal oxide, the metal oxide is positively charged. The charged surface and surrounding solution form a thin double layer, to which oppositely charged ions are attracted and initial reaction proceeds. The PZC of the TiO_2 is reported to be in the range of 5.5–6.0 [30], resulting in a negatively charged surface in the coating solution (The pH was measured of 6.50 in this investigation). When the positively charged Ca^{2+} is attracted to the surface of Ti6Al4V alloy, it reacts with the TiO_2 to form $CaTiO_3$, the PZC of which was reported as 8.1 [31], causing the $CaTiO_3$-covered surface to be positively charged and the PO_4^{3-} attracted to the surface to participate in further reactions, leading to the formation of calcium phosphate.

The results of EDX point analysis (Fig. 8b) on the hydroxyapatite coating and corresponding ratios of Ca/P are listed in Table 3. Measurements 3 and 4 close to the substrate show the coexistence of Ca, Ti, V or P, indicating a preferential formation of Ca on the Ti6Al4V surface at the initial stage of deposition (no phosphor was detected in measurement 3). The phosphor then participates in subsequent deposition, as is evident in measurement 4, away from the substrate surface. In summary, EDX point analysis confirms the existence of initial diffusion layer and the sequential participation of Ca^{2+} and PO_4^{3-} in the formation of HA coating.

With the formation of calcium phosphate apatite on the surface, the super-saturation of simulated physiological solution may promote preferential nucleation of apatite on the already-formed apatite rather than in the solution, the formed hydroxyapatite acts as seeds to accelerate the formation of the hydroxyapatite [32, 33]. Thus the further formation of the apatite coating continues on the initial apatite layer by spontaneous growth consuming calcium and phosphate ions from the surrounding simulated body fluid. A theoretical analysis [34] also indicates that formation of hydroxyapatite exhibits a higher thermodynamic preference than that of octacalcium phosphate (OCP) and dicalcium phosphate (DCPD). Thus the further formation of the coating proceeds in the form of hydroxyapatite, rather than OCP or DCPD. This effect is evident by the eventual formation of hydroxyapatite shown by measurements 1, 2 and 5, which are away from the initial deposition layer and the substrate. The average of Ca/P ratios of these three measurements is 1.67, which is exactly the atomic ratio of Ca/P in stoichometric hydroxyapatite ($Ca_{10}(PO_4)_6(OH)_2$).

3.3.2 *FTIR, XRD and TEM characterization of coating*

XRD analysis (Fig. 9) of a commercial crystallized hydroxyapatite powder (PENTAX Corporation, Tokyo, Japan) and the comparison with the powders of formed coating confirms that the formed coating is hydroxyapatite. The commercial HA XRD patterns (lower curve) match very well with the standard XRD pattern of HA in the JCPDF card, major patterns of the coating powders (upper curve) are shown and match with the commercial HA powders.

Figure 10 is the FTIR spectra at different duration of coating process. The spectra show the characteristic bands of hydroxyapatite along with additional bands of associated H_2O. It is concluded that the formed apatite coating is hydroxyapatite, consistent with the XRD analysis.

The stretching vibration of PO_4^{3-} can be observed in the range of 1,200–900 cm^{-1}, which in this investigation

Table 3 EDX analysis (atomic percentage) on the cross-section of coating

	Measurement	C	O	P	Cl	Ca	Ti	V	Ca/P	Average
Initial Layer	3	21.80				21.47	51.55	5.19	N/A	N/A
	4	32.71	25.72	5.25		21.47	13.68	1.23	4.08	
Bulk Coating	2	58.04	18.72	8.33	0.56	14.35			1.72	1.67
	5	64.56	18.11	6.36	0.36	10.59			1.67	
	1	67.77	16.43	5.81	0.52	9.47			1.63	

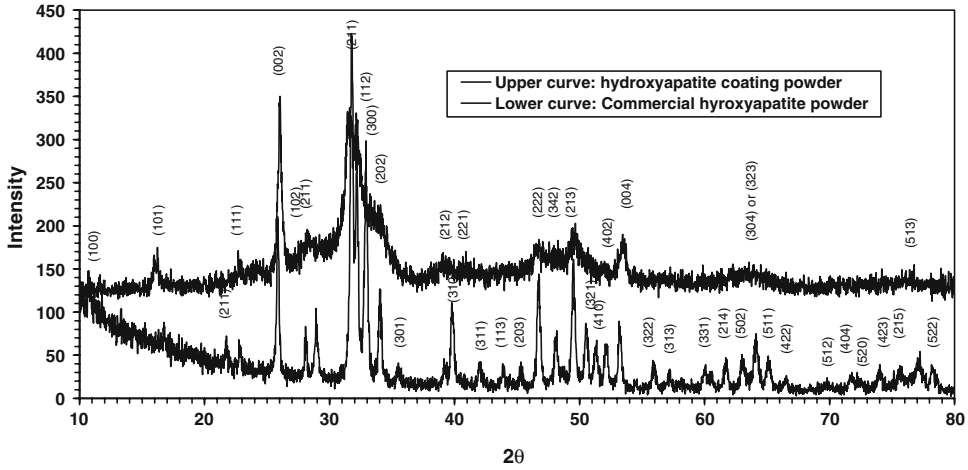

Fig. 9 XRD analysis of a commercial HA powder and powder of formed coating

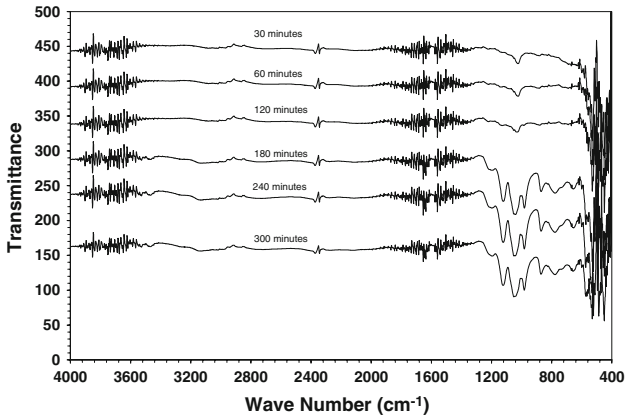

Fig. 10 FTIR spectra of coatings at different durations

located at 1,119, 1,048, 1,036 and 979 cm^{-1}; the deformation vibration of PO_4^{3-} are located at the bands of 603, 572, 471 and 422 cm^{-1}; as for hydroxyl (OH^-), the bands are located at 3,458 and 617 cm^{-1}. The fluctuations located in the range of 3,900–3,500 and 1,900–1,400 can be assigned to the associated H_2O in the coating, a possible result of long period exposure of porous HA in the atmosphere. The intensities of the hydroxyapatite bands are significantly increased with the increasing duration of coating.

The broad characteristic bands of HA illustrate amorphous or poorly crystallized phases of initially deposited HA during the first 120 min. The bands split after 180 min deposition shows that the formed HA is gradually crystallized, but still not fully crystallized due to the relative broadness of the band peaks. The sharpness of bands, especially that of the 572 and 601 cm^{-1} bands, indicates a well-crystallized HA.

Figure 11a is the TEM diffraction patterns of the formed HA coating, showing that the formed HA coating has crystal structure and the measured d-spacings match with that of pure HA (corresponding d-spacing numbers for pure HA are 4.72, 3.51, 3.17, 2.81, 2.53, 2.30, 1.89, 1.59, 1.50, 1.43, 1.35). The formed HA coating has nanoscale grain size of less than 20 nm, the crystal planes are shown inside the grains and corresponding d-spacing can be measured (Fig. 11b). Morphologies of a single HA plate also show that the grain is less than 20 nm in size (Fig. 11c).

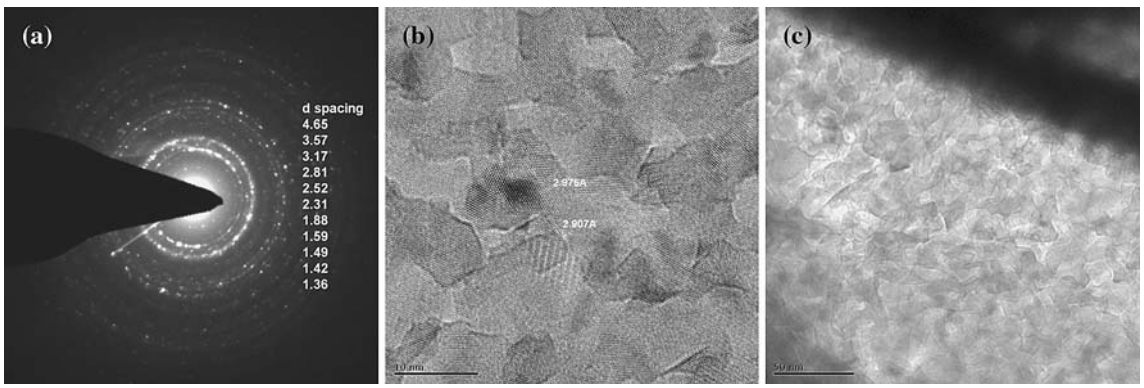

Fig. 11 TEM analysis of formed coating in terms of (**a**) diffraction pattern, (**b**) grin size and crystal planes, and (**c**) morphology of grains

4 Conclusions

A novel HA coating process is developed to deposit hydroxyapatite coating with porous bone-like structure on Ti6Al4V alloy. This method is capable of producing uniform deposit due to its non line-of-sight nature. The deposition proceeds through heterogeneous nucleation on the activated substrate due to the biocompatible TiO_2 and favorable surface chemistry created through the electrochemical activation in NaOH solution. Growth of the coating from a replenished solution is linearly related to the coating duration and reaches 50 μm within 15 h. The formed coating resembles the porous bone-like features of the electrochemically activated substrate, and is characterized as pure hydroxyapatite using XRD and FTIR analysis. Further, the deposit features nano-scale grain size.

Acknowledgements The authors gratefully acknowledge the funding support from the CIHR-NRC Science and Technology Convergence Program for Innovation. Thanks are also given to Professor W. K. Wan from the University of Western Ontario for his help in FTIR analysis.

References

1. R. Bourne, C. Rorabec, J. Patterson, J. Guerin, Clin. Orthop. **393**, 112 (2001)
2. H. Kawamura, M. Dunbar, P. Murray, R. Bourne, C. Rorabeck, J. Bone Joint Surg. **83A**, 1333 (2001)
3. A. Campbell, C. Rorabeck, R. Bourne, D. Chess, L. Nott, J. Bone Joint Surg. Br. **74**, 63–66 (1993)
4. R. Bourne, C. Rorabeck, M. Ghazal, M. Lee, J. Bone Joint Surg. Am. **76**, 1464–1470 (1994)
5. J. Lausmaa, B. Kasemo, H. Mattsson, Appl. Sur. Sci. **44**, 133–146 (1990)
6. E. Mccafferty, J.P. Wightman, Appl. Surf. Sci. **143**, 92–100 (1999)
7. J. Pouilleau, D. Devilliers, F. Garrido, S. Durand-Vidal, E. Mahé, Mater. Sci. Eng. **B47**, 235–243 (1997)
8. D.M. Brunette, P. Tengvall, M. Textor, P. Thomsen, *Titanium in medicine* (Springer-Verlag, Berlin, Heidelberg, New York, USA, 2001) p. 5
9. H.M. Kim, F. Miyaji, T. Kokubo, T. Nakamura, J. Biomed. Mater. Res. **32**, 409–417 (1996)
10. K. Hata, T. Kokubo, J. Am. Ceram. Soc. **78**, 1049–1053 (1995)
11. Y. Tang, Y. Liu, U. Sampathkumaran, M.Z. Hu, R. Wang, M.R. de Guire, Solid State Ionics **151**, 69–78 (2002)
12. T.M. Lee, B.C. Wang, Y.C. Yang, E. Chang, C.Y. Yang, J. Biomed. Mater. Res. **55**, 360–367 (2001)
13. S.J. Ding, C.P. Ju, J.H.C. Lin, J. Mater. Sci. Mater. M **11**, 183–190 (2000)
14. S. Hayakawa, A. Osaka, J. Non-Cryst. Solids **263 & 264**, 409–415 (2000)
15. J. Wang, P. Layrolle, M. Stigter, K. de Groot, Biomaterials **25**, 583–592 (2004)
16. L. Jonášová, F.A. Müller, A. Helebrant, J. Strnad, P. Greil, Biomaterials **25**, 1187–1194 (2004)
17. A. Stoch, A. Brożek, G. Kmita, J. Stoch, W. Jastrzębski, A. Rakowska, J. Mol. Struct. **596**, 191–200 (2001)
18. H.W. Kim, Y.H. Koh, L.H. Li, S. Lee, H.E. Kim, Biomaterials **25**, 2533–2538 (2004)
19. F. Barrere, M.M.E. Snel, C.A. van Blitterswijk, K. de Groot, P. Layrolle, Biomaterials **25**, 2901–2910 (2004)
20. A.C. Tas, Biomaterials **21**, 1429–1438 (2000)
21. L.B. Kong, J. Ma, F. Boey, J. Mater. Sci. **37**, 1131–1134 (2002)
22. J. Xie, B. Luan, J. Biomed. Mater. Res. **84A**, 6372 (2008)
23. T. Kokubo, Acta Mater. **46**, 2519–2527 (1998)
24. Q.L. Feng, H. Wang, F.Z. Cui, T.N. Kim, J. Cryst. Growth. **200**, 550–557 (1999)
25. H.B. Wen, J.G.G. Wolke, J.R. de Wijn, Q. Liu, F.Z. Cui, K. de Groot, Biomaterials **18**, 1471–1478 (1997)
26. F. Liang, L. Zhou, K. Wang, Surf. Coat. Technol. **165**, 133–139 (2003)
27. K. Hata, T. Kokubo, J. Am. Ceram. Soc. **78**, 1049–1053 (1995)
28. F. Barrere, P. Layrolle, C.A. van Bliterswijk, K. de Groot, Bone **25**, 107S–111S (1999)
29. F. Li, Q.L. Feng, F.Z. Cui, H.D. Li, H. Schubert, Surf. Coat. Technol. **154**, 88–93 (2002)
30. M. Kosmulski, J. Colloid Interf. Sci. **253**, 77–87 (2002)
31. T. Hanawa, M. Kon, H. Doi, H. Ukai, K. Murakami, H. Hamanaka, K. Asaoka, J. Mater. Sci. Mater. M **9**, 89–92 (1998)
32. R.I. Martin, P.W. Brown, J. Biomed. Mater. Res. **35**, 299–308 (1997)
33. W. Wu, H. Zhuang, G.H. Nancollas, J. Biomed. Mater. Res. **35**, 93–99 (1997)
34. X. Lu, Y. Leng, Biomaterials **26**, 1097–1108 (2005)